Potential of Using Simulated Data in Processing Photoacoustic Measurement Data

M. I. Jordovic Pavlovic, A. D. Kupusinac, S. P. Galovic, D. D. Markushev, M.N. Nesic, K.Lj.Djordjevic, M. N. Popovic

Abstract: This paper explores the potential of using simulated data in calibration of photoacoustic measurement system. The database of simulated experimental values is created using software developed on the bases of the theory-mathematical model. Reliability of the data was gained thanks to the expert knowledge. An artificial neural network as a precise prediction tool is trained on the developed database of simulated data to recognize type of the microphone used as a detector in photoacoustic experiment. The result is classification model satisfies the basic requirements of a photoacoustic experiment: accuracy, reliability and real time operations. The paper discusses the optimization of classification model in terms of used computational power, required precision and process rate in relation with defined problem. The obtained results justify the idea of using simulated data in photoacoustic. Presented theory-mathematical model and classification model are part of developed machine learning framework for processing photoacoustic measurement data.

Keywords: Machine learning, artificial neural networks, simulated data, classification, photoacoustics, microphone

I. Introduction

Machine learning techniques are considered suitable tool for intelligent decision making, and therefore they have found application in various domains. When input and output parameters are linked with some kind of pattern, and sufficient data is available, this pattern can be discovered or approximated by machine learning algorithm being trained on that same data. Subsequently, output for particular inputs outside the learning dataset can be calculated (with more or less accuracy) using this newly discovered pattern. This means that if the quality and the quantity of the data used for learning are sufficient, and the discovered pattern also exists for events that were not part of the learning dataset, the produced result can be used to approximate the outputs based on any future input[1]. Machine learning algorithms, and, in particular, artificial neural networks (ANN), are frequently used as reliable and fast prediction tools. They are often used in photoacoustics (PA), a popular method in photothermal (PT) science in the last few years, for: noise removal in photoacoustic recognition of images [2], simultaneous determination of the laser beam spatial profile and relaxation time of the polyatomic molecules in gases in real time within the trace atmosphere gases monitoring [3][4], reconstruction of optical profile of optically gradient materials based on frequency, magnitude and phase of measured PT response [5], etc.

In this paper, a few of the several results achieved in PA measurement system characterization research are presented. The ultimate goal is material characterization. The aim of the PA measurements is the determination of physical properties (thermal, optical, mechanical, elastic, electronic and other related ones) of the examined structure from its PA response. All PT methods are indirect measurement techniques, and so is the photoacoustics, meaning that these methods are model dependent. In terms of mathematics, obtaining physical properties by these methods is considered an inverse problem that can be assessed in two steps:

1. **Development of the direct (forward) model – direct solution of the inverse problem,** i.e. developing the mathematical model that sufficiently well describes physical processes leading from the optical excitation to the thermal response. First step is theoretical-mathematical modeling of temperature distribution within the sample, on front and back sample surfaces and in its surroundings, and then theoretical-mathematical modeling of the specific PT response (in this case the PA response)

2. **Development of the inverse procedure – inverse solution of the inverse problem,** i.e. the determination of physical properties of the sample based on measured photothermal response, developed mathematical model and well known preset of input parameters (the intensity and modulation frequency of the incident optical radiation). Some of the inverse procedures are fitting, numerical procedures and neural networks. Fitting and numerical procedures are time consuming procedures, demanding the engagement of the researcher. These are drawbacks regarding scientific and further industrial application of the method, where a real time procedure is appreciated. The reasonable choice is

Miroslava Jordović Pavlović is with the Western Serbia Academy of Applied Studies, Užice, Trg Svetog Save 34, 31000 Užice, Serbia (miroslava.jordovic-pavlovic@vpts.edu.rs).

Aleksandar Kupusinac is with Faculty of Technical Sciences, University of Novi Sad, 6 Trg Dositeja Obradovića, 21000 Novi Sad, Serbia (sasak@uns.ac.rs).

Slobodanka Galović is with the Vinča Institute of Nuclear Sciences, 12-14 Mike Petrovića Alasa, 11351 Vinča, Serbia (bobagal@vin.bg.ac.rs).

Dragan Markushev is with the Institute of Physics, University of Belgrade, Pregrevica 118, 11080 Pregrevica, Serbia (dragan.markushev@ipb.ac.rs).

Mioljub Nešić is with the Vinča Institute of Nuclear Sciences, 12-14 Mike Petrovića Alasa, 11351 Vinča, Serbia (mioljub@gmail.com).

Katarina Đorđević is with the Faculty of Physics, University of Belgrade Studentski trg 12, 11000 Beograd, Serbia (katarinaljdjordjevic@gmail.com).

Marica Popović is with the Vinča Institute of Nuclear Sciences, 12-14 Mike Petrovića Alasa, 11351 Vinča, Serbia (maricap@vin.bg.ac.rs)

artificial neural networks as a very efficient machine learning algorithm. Because of the complexity of the inverse problem more than one ANN is needed.

Firstly, the characterization of the sample and the prediction of its thermal, mechanical and optical properties based on its PA response, require the use of one ANN. This is already done in [6]. But the necessary precondition is that the PA response in use is influenced only by the sample, which, unfortunately, is not the case. The PA response is non- linearly affected not only by the sample but also by the measurement instrument chain and the appearing noise. So, the PA response has to be corrected first, in order to obtain the so called "true" signal. In the first preprocessing procedure that was developed, noises are removed during data acquisition. In the second preprocessing procedure, calibration of the measurement system has to be done. Because of the dominant impact of the microphone on the distortions in the measurement instrument chain, as the consequence of using minimum volume cell configuration of the PA experimental set-up, calibration of the measurement system boils down to the calibration of the microphone. The key of this brand new idea is the determination of microphone transfer function. Furthermore, the division of PA response amplitude data by corresponding microphone characteristics and its subtraction from the PA response phase data will result in gaining the so called "true" signal, originating only from the sample. Unfortunately, microphone specifications provided by the manufacturer are not precise enough, particularly in the case of phase transfer function. Besides, microphone cavity is not considered as the source of resonances, which is inevitable in PA measurements. Since, these specifications could not be used, the other solution is needed. Non-linear influence of the microphone on a PA response suggests ANN application. Having in mind that ANN seeks large datasets (is data hungry) [7], the first requirement for the application of neural networks is set. But this requirement is opposed to two facts related to PA measurements: firstly, such a numerous experimental collection is very difficult to obtain, and secondly, based on the experience, real experimental data can hide a very serious problem of the influence of the measurement system on the estimated parameter values [8]. Therefore, another solution for database creation is presented: the idea of theoretical-mathematical model as a base for designing a software for the simulation of PA experimental values. Thanks to the developed software, amplitude and phase data of the simulated PA response are obtained. Here, satisfactory credibility to the experiment is of essential importance in order to make the newly created method precise enough. Therefore, expert knowledge (i.e., the preset input parameters) is crucial for the solution of this problem.

Simulated data have often been used for training in machine learning problems in the past few years [9][10][11], but as far as we know, the idea of using simulated experimental values, obtained by developed software based on a theoretical - mathematical model, for training a machine learning model is new. This article presents a few steps of a complex correction procedure performed in photoacoustic measurements. Firstly, a complete method of making a large amount of reliable simulated data as a precondition for applying neural networks as the inverse solution of the inverse problem is explained. Secondly, a process of designing classification model for microphone type recognition as the first step in recognizing measurement system characteristics is discussed on the base of optimal computational complexity, required precision and process rate in relation to the given problem and available data set. Classification of microphone type will determine the shape of the transfer function and the levels of signal exaggeration and attenuation. Once the class of the microphone is defined, characterization of microphone will be simplified by limiting the database made for various types of microphones to a database of a particular microphone type. This idea is presented in our previous work [12]. That way, time, and computational power are saved, which are real benefits of the classification model. Learning on the defined database of classified microphone type, ANN based model for microphone characterization [13] predicts characteristic microphone parameters with satisfying accuracy, which together with the corresponding shape, precisely determine microphone transfer function [12].

This paper shows that if a massive dataset is obtained and the quality of data is high, less computation power is needed, and higher process rate is gained for the solution of machine learning problem.

II. THEORETICAL -MATHEMATICAL MODEL OF PHOTOACOUSTIC RESPONSE

Photoacoustics, as one of photothermal methods, is based on the photothermal effect. The photothermal effect is the effect of generation of heat as a consequence of the absorption of the incident electromagnetic radiation, from a wide spectrum of wavelengths, in different relaxation and de-excitation processes. This way generated heat causes the disruption of the thermodynamic state of the sample (pressure, temperature, density) which propagates through the sample and the nearby environment, producing a number of detectable phenomena. In photoacoustics, the first and the most used photothermal method, a sample is placed inside the photoacoustic cell that contains air and microphone. It is exposed to a modulated light beam which causes periodic sample heating. As a consequence, the air pressure in the PA cell oscillates, which can be detected by a microphone [14].The photoacoustic cell can be designed in a so called "reflection configuration", with the source and the microphone set up on the same side of a sample, or the "transmission configuration", where a sample is placed between the source and the microphone. In our experimental set up, the minimum volume cell configuration is employed. It is kind of transmission cell configuration where sample is mounted directly on the top of the microphone, instead of the dust cover, as presented in figure 1, [15]. This way, the microphone chamber acts as the PA cell, closed by the sample on one side and the microphone diaphragm on the other one, which causes disruptions of the recorded signal on its endings [16].

Power levels of experimentally recorded signals are, generally, low. In order to make the level of the recorded signal higher than the level of the noise (real – flicker noise, coherent signal deviation and random noise), the absorption of the sample has to be large. In the case of materials with significant reflection, the additional coating is needed, while in the case of transparent (or semitransparent) samples, the coefficient of transmission has to be augmented. However, due to high level of transmission, the absorption of the incident radiation in the surrounded air can`t be neglected and the recorded signal begins to contain unnecessary information. The problem is even bigger in the case of the minimum volume cell configuration, where the microphone has to be protected because of the small dimensions of the cell. Another solution is, also, an additional layer of high absorption.
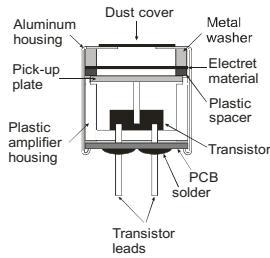

Fig. 1. Experimental setup

Photoacoustic response within the transmission configuration is the sum of two dominant signal components: thermoconducting and thermoelastic component. Thermoconducting component arises due to the periodic heat flow from the sample to the surrounding gas (thermal-piston effect) and thermoelastic component arises due to the thermoelastic banding of the sample (drum effect) [17][18][19][20][21][22][23][24][25].

In our experiments two-layer structure is employed. The first layer is black coating, and the second layer is the investigated sample. Theoretical-mathematical model of PA response of a two-layer system, used for obtaining the dataset, is given by following expressions [26][27]:

$$\tilde{p}_{tot} = \tilde{p}_{th} + \tilde{p}_{ac} \qquad (1)$$

$$\tilde{p}_{th} = \delta P = \frac{\gamma P_0}{l_g T_0} \frac{1}{\sigma_g} \vartheta(l_s) \qquad (2)$$

$$\tilde{p}_{ac} = \frac{3\gamma P_0}{l_a} \frac{R^2}{l_s^3} \left[\alpha_{T1} \int_0^{l_1} \left(x - \frac{l_s}{2} \right) \tilde{\vartheta}(x) dx \right. \qquad (3)$$

$$\left. + \alpha_{T2} \int_{l_1}^{l_s} \left((x - l_1) - \frac{l_s}{2} \right) \tilde{\vartheta}(x) dx \right]$$

Where p_{tot} is total pressure that we want to record by photoacoustic, p_{th} is the thermoconducting component and p_{ac} is the thermoelastic component. Furthermore P_0 is the presser in the cell, V_0 is the volume of the cell (in the case of the minimum volume cell V_0 represents the volume of the chamber cavity), γ represents the heat capacity ratio, α_T is the thermal expansion coefficient, R_c is the radius of the chamber in front of the microphone diaphragm, l_1 and l_2 are the thicknesses of the first and second layer, while l_s is the sum of the thicknesses these two layers (l_1 and l_2). $\vartheta(x)$ represents temperature variations inside the samples and $\vartheta(l_s)$ is the surface temperature variation on the rare surface. Expressions for these

temperature variations are given in the article [28][29]. The presented model described the total presser as photoacoustic response, and its components in the two-layer system surrounded by the air and it is based on the Generalized model of heat conduction that implies finite heat propagation speed. The system depicts volume absorption of incident optical beam in both layers [26][27][28][29].

Appearance of amplitude and phase characteristics of the theory-mathematical simulated total pressure are shown on figure 2a) and 2b) respectively.
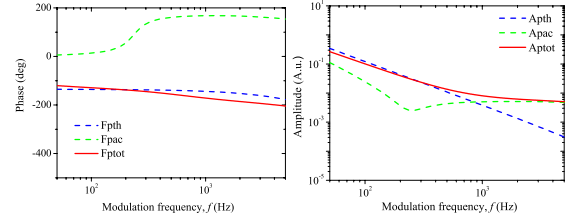

Fig. 2 Simulated amplitude and phase (solid line) of the total photoacoustic signal, $p_{tot}(f)$, as a function of the modulation frequency f, together with the appropriate components $p_{th}(f)$ and $p_{ac}(f)$ (dotted lines).

In a minimum volume cell PA experiment [30], microphone is the fundamental part of the detector system. Microphone is an acoustic-electric converter, but its transfer function in frequency and time domain differ due its construction, applied geometry and membrane type. In the literature [8] and in our experimental experience, microphone behavior is described as filtering. At low frequencies (< 1 kHz), electret microphones (commonly used in PA) usually act as electronic high-pass filters, while at high frequencies (> 1 kHz) these microphones usually act as acoustic low-pass filters.

The influence of the measurement chain, including the microphone as the component that has the greatest impact in signal distortion, is given by the following mathematical expressions describing total transfer function:

$$H_1^e(f) = \frac{1}{1 - j\frac{f_1}{f}} \qquad (4)$$

$$H_2^e(f) = \frac{1}{1 - j\frac{f_2}{f}} \qquad (5)$$

$$H^a(f) = \frac{f_3^2}{f_3^2 - f^2 + jff_3\xi_3} + \frac{f_4^2}{f_4^2 - f^2 + jff_4\xi_4} \qquad (6)$$

$$H_{mic}(f) = H_2^e(f)H_{total}^a(f) \qquad (7)$$

$$H_{total}(f) = H_1^e(f)H_{mic}(f) \qquad (8)$$

In previous equations, $H_1^e(f)$ represents electronic characteristic of the influence of the other components in the measurement chain, first of all the sound card, and f_1 is the characteristic frequency that describes this system. Based on experimental experience, it is assumed that this frequency is constant. $H_2^e(f)$ and $H^a(f)$ represent electronic and acoustic characteristics of the microphone. f_2 correspondes to the characteristic frequency of the electronic high-pass filter and f_3 and f_4 to the characteristic frequencies of the acoustic low-pass filters of the microphone, ξ_3 and ξ_4 are reciprocial values of the quality factor, or, in other words, the double value of the damping factor. The product of these two components represents the microphone response. As a consequence, the microphone response in frequency domain is deviated in

amplitude and phase, especially at the begging and at the end of frequency range. Different microphone types have different transfer functions, but transfer functions of two microphones of the same type are usually different, because, in practice, two identical microphones do not exist. Theoretical-mathematical model for the total photoacoustic signal recorded by the minimum volume cell photoacoustic experimental set up represents product of the total pressure and the total transfer function:

$$S(f) = \sigma p_{total}(f) H_{total}(f) \qquad (9)$$

Based on this equation and numerical simulations of the experiments, the database is obtained. Amplitude and phase data of the simulated PA response are given in figure 3a) and 3b). All the curves (amplitude and phase) of distorted photoacoustic signal have expected shape, according to experimental experience. There are no outliers.
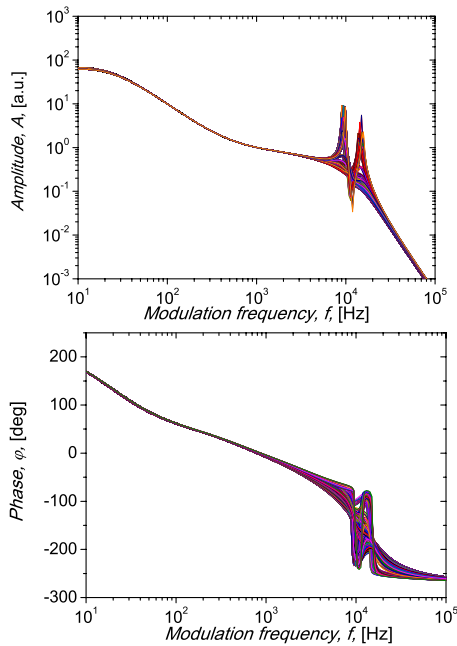

Fig. 3 Curves a) amplitude and b) phase of distorted photoacoustic signals with different microphone characteristics from the dataset used for network training[12]

III. DATABASE DESCRIPTION

Based on theoretical-mathematical model, software for creating simulated experimental values or numerical experiments is designed using programming IDE of Matlab. Microphone theoretical characteristics, corresponding to commercially available microphones ECM30B, ECM60 and WM66, are given in Table 1. Beside these microphone types, frequently used in PA experiments, simulations for another type of microphone are created, the so called ideal microphone (IM). Considering ideal microphone is of great importance for the correction procedure. If a microphone exerted ideal behavior, meaning it had flat PA response, that would mean that measurement chain would be equally sensitive in the whole frequency domain, so the correction procedure would be unnecessary. So, taking IM into account, we are saving the time.

	Dye	Aluminum
Thermal conductivity [Wm^{-1}K^{-1}]	70	210
Thermal diffusivity [m^{2}s^{-1}]	2.5×10^{-5}	8.6×10^{-5}
Thermal relaxation time [s]	10^{-4}	10^{-12}
Absorption coefficient [m^{-1}]	10^8	145×10^6

During the process of the examination, the black dye-aluminum structure was investigated. Aluminum plate, 197 μm in thicknesses and with radius of 10 μm was covered in black ink dye, 2 μm in thicknesses. Thermal, thermal memory and optical parameters used for obtaining database are given in Table 1.

Expert knowledge was crucial in obtaining similarity good enough with the experiment. Based on experimental experience, characteristic microphone parameters are considered to have different stability, regarding the reproducibility in each measurement. Accordingly, different value ranges were set for different parameters. Frequency f_2 is the most stable parameter due to its origin from RC microphone characteristic, so three values ware taken for network training: central value $f_{20} = 25$ Hz for the microphone ECM30B and two values which are ± 5 % apart from the central value (23.75 Hz and 26.25 Hz). By analogy, the values for the ECM60 are: 14.25Hz, 15Hz and 15.75 Hz, for the WM66 they are: 61.75 Hz, 65 Hz and 68.25 Hz, while for IM the values are: 0.475Hz, 0.5 Hz and 0.525 Hz. Frequencies f_3 and f_4 are more dependent on experimental conditions then f_2, so they are less stable than f_2. Ten values, equally distanced in the corresponding ranges, were considered to be good enough for the description of experimental behavior related to those two frequencies. f_{30} is taken in the range 8930-9866 Hz and f_{40} is taken in the range 13965-15432 Hz for ECM30B. Microphones ECM60 and WM66 have the same ranges for frequencies f_3 and f_4, 7980-8817 Hz and 13015-14383 Hz respectively. For IM f_3 is in the range of 190000-209998 Hz while f_4 is in the range of 285000-314997 Hz respectively. Damping factors of the second order low-pass filter ξ_3 and ξ_4 are strongly dependent on experimental conditions and they are the most unstable parameters. Each value range, for ξ_3 and ξ_4, was chosen based on the peak appearing in the amplitude characteristic of the second order filter. Critical value of quality factor in the case of limitary situation where signal is extremely damped and respectively unforced is Q=0.5. Significant change happens from Q=1 to Q=100 hence $\xi \in [0.99, 0.015]$. 15 values, irregularly distributed in this range, were taken for the each type of microphone. This kind of microphone parameter distribution was assumed to be good enough to simulate all possible experimental situations. The discussion and comparison of inverse problem-solving concepts in photoacoustics is presented in our previous work [31]. There are 65,000 paired curves for each microphone type, as 65,000 simulated experimental results, and those are 65,000 records of the database. Paired curves (two curves) mean that there are both amplitude and phase data for the given set of microphone parameters. Each curve contains data sampled at 200 frequency values in the range from 10Hz to 100kHz. By taking such a

wide frequency domain, the possibility of using microphones with different membrane material (mylar, nickel, graphene) is considered. In total, every record is represented with 400 samples, 200 samples of amplitude and 200 samples of phase characteristics. Those are features for our machine learning problem. In other words each frequency is presented with two features, sample of amplitude and sample of phase, so we have resolution of two for every point on frequency axes. At the end of each database record, the information about which microphone type a particular record belongs to is written. The classification problem has 4 classes of microphones, symbolically presented with 0, 1, 2 and 3.
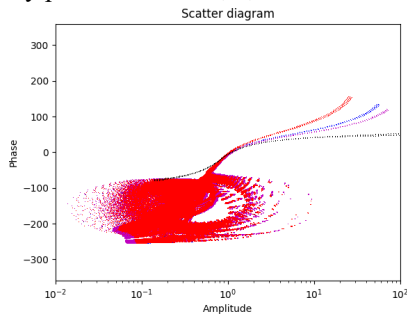

Fig.4. Visualization of the data, different colors correspond to different microphone types

Visualization of the data used in classification modeling, the form of scatter diagram, is given in Fig. 2. Each point on a scatter diagram is one point of 200 points that corresponds to one curve of 270,000 curves in the database. Different classes of microphone are presented with different colors. Analyzing the diagram, one can conclude that points are completely classified to four classes or four microphone types in upper-right part of the diagram, meaning for certain distribution of amplitude and phase values it is clear to which class point belongs. That distribution of amplitude and phase values are happening in a low frequency domain. In lower-left part of the diagram points are mixed, meaning that for that distribution of amplitude and phase values it is not clear to which class point belongs, i.e. curves (or classes) overlap. Thus, classification model has more difficult task because of the overlap. Training, validation and test sets are obtained randomly because dataset is first shuffled and then divided into training, validation and test set. Generalization of the results is obtained on that way, thus 243 000 records or 90% of the total number of records belongs to the training set, 13500 records or 5% belong to the validation set and the rest belongs to the test set.

IV. RESEARCH RESULTS AND DISCUSSION

Once, the topology of the model is chosen, the next step is fine-tuning of topology itself, parameters and hyperparameters of the model. It is done in iterative process idea-code-experiment, with a numerous attempt using literature suggestions [32][33] and experience.

In pre-processing step, data scaling was done by performing the normalization of the input and output. Max normalization was chosen. It means that each element x_i of the input vector is divided by its maximum absolute value, which is the maximum of absolute values of all the samples, a total of 270000 values, at the i-th frequency. In other words, it is absolute maximum value of the i-th row of the input matrix. This way normalization of the input vector is done, all the values of the input vector are equal or less than unity. Similarly, normalization of the output vector is done. For weights parameters initialization, among others Xaviar algorithm [34] is chosen. The activation function *tanh()* is used for forward propagation and the Adam algorithm [35] is used for the optimization of weights in backpropagation. The optimization is intensified by the Mini-batch technique, size of 128. Because of the classification function softmax in the last layer, a cross entropy with logits is used as the error function and system performance measure during training. Neural network tuning on number of hidden layers and the number of neurons is presented in Table 2.

TABLE II
NUMBER OF HIDDEN LAYERS AND NUMBER OF NEURONS IN HIDDEN LAYER(S) ANALYSES

No.of hidden layers	1	2	2	2	1	2
No. of neurons of the 1. h. l.	10	8	7	9	5	3
No. of neurons of the 2. h. l.	/	2	3	1	/	2
Train accuracy(%)	99.99	99.99	99.99	75.02	99.99	99.99
Dev accuracy(%)	99.99	99.99	99.99	74.15	99.99	99.99
Test accuracy(%)	99.99	99.99	99.99	75.45	99.99	99.99
Number of epochs	100	100	100	100	100	100
Prediction time (ms)	14.34	17.89	17.44	/	14.06	16.75

2	1	2	2	1	2	1
4	4	2	3	3	2	2
1	/	2	1	0	1	0
50.03	99.99	99.99	81.15	99.99	75.01	99.99
49.19	99.99	99.99	82.09	99.99	75.03	99.99
50.15	99.99	99.99	81.11	99.99	74.7	99.99
100	100	100	100	100	100	100
/	13.89	16.89	/	13.73	/	13.93

According to Table 2, for the defined classification problem and the dataset of 270000 records following conclusions can be drawn. One neuron in second hidden layer in configuration of two hidden layers is not appropriate and those topologies were dismissed, but 2 neurons in second hidden layer are satisfying. The reason are 4 classes at the output. There is no difference in accuracy in the case of the configuration with one hidden layer and in the case of configuration with two hidden layers with same total number of neurons. Based on experimental experience one can say that for other machine learning problems that was not a case. This is specificity of this particular problem. So, the topology and the choice of model parameters and hyperparameters are singularity of machine learning problem and the quantity and quality of available data. Minimum configuration that satisfies required accuracy is one hidden layer with 2 neurons. It is surprisingly small number of neurons, which can be justified with the large data set. It means that learning with large datasets decreases the number of computational units of ANN configuration, it becomes computationally simpler. Large dataset brings into the model huge knowledge about the problem, in the case of our classification problem knowledge about photoacoustic experiment environment. Using this knowledge ANN needs less computational power and less epochs for learning. Analyzing the obtained prediction time of different topologies of classification model, the most important influence on the processing rate has the number of hidden

layers, the number of neurons in layer has minor influence, even if there is significant difference in the number of neurons.

Concerning the prediction, the network gives very high accuracy, train, dev and test accuracy are equal, 99.99%. Concerning the training, the network obtained good results even for very quick training, that lasts 100 epochs. According to the equal values of training, dev and test accuracy and low error function on the new data sets we can conclude that the network generalizes very well. There is no overfitting.

The reliability of the model was tested on simulated data. Sixteen different independent datasets, meaning four different amplitude and phase characteristics for each type of microphone were created, where the microphone parameter values differed from those on which the network was trained, but in the given parameter range. Results are presented in Table 3. According to Table 3 our model is reliable, it recognizes the microphone type precisely and gives an answer regarding the microphone type in real time.

Results of the model on real experimental data are presented in [12].

TABLE III
RESULTS OF INDEPENDENT TESTS

Test	1	2	3	4	5	6	7	8	9	10	11	12	13	14	15	16
Class.	1	3	0	2	1	2	3	0	2	3	1	2	1	0	3	0
Accuracy	✓	✓	✓	✓	✓	✓	✓	✓	✓	✓	✓	✓	✓	✓	✓	✓

V. CONCLUSION

In this paper a complete explanation of the necessity for simulation data in the processing real photoacoustic measurement data is given. Software for simulations is designed based on the presented theoretical-mathematical model, while the credibility to the experiment is obtained using expert knowledge. Classification model for microphone type recognition is trained on the obtained database. Because of the huge, reliable dataset, knowledge about the photoacoustic experiment is embedded in the classification model so it could be optimized to a pretty simple topology, while the learning process was extremely efficient. In terms of precision and real time processing, classification model satisfies requirement of the photoacoustic experiment. In terms of reliability, classification model did not make any mistake in tests maintained with simulated data. The benefits of the presented model for PA measurements are multiple. By recognizing the microphone type the shape of transfer function and levels of signal exaggeration or attenuation are determined and that will simplify the further procedure of recognition of microphone characteristics in order to deprive PA signal of instrumental deviations. If the recognized microphone has flat characteristics the correction procedure is skipped. In the case of shaped response the correction procedure is done using only database of recognized microphone instead of whole database for all types of microphone. The processing time is saved this way. The generality of the model could be accomplished by extending the number of microphone types if such requirement of the experiment exists. In the future, we intend to explore modeling of noise distribution to generate data similar to real data and skip the first step of correction procedure, the noise removal.

REFERENCES

[1] Y. S. Abu-Mostafa, M. Magdon-Ismail, and H.-T. Lin, *Learning From Data*. AML Book, 2012.

[2] D. Allman, A. Reiter, and M. A. L. Bell, "Photoacoustic Source Detection and Reflection Artifact Removal Enabled by Deep Learning," *IEEE Trans. Med. Imaging*, vol. 37, no. 6, pp. 1464–1477, 2018.

[3] M. Lukić, Ćojbašić, M. D. Rabasović, D. D. Markushev, and D. M. Todorović, "Laser Fluence Recognition Using Computationally Intelligent Pulsed Photoacoustics Within the Trace Gases Analysis," *Int. J. Thermophys.*, vol. 38, no. 11, 2017.

[4] M. Lukić, Ž. Ćojbašić, M. D. Rabasović, and D. D. Markushev, "Computationally intelligent pulsed photoacoustics," *Meas. Sci. Technol.*, vol. 25, no. 12, p. 125203, 2014.

[5] M. N. Popovic, D. Furundzic, and S. P. Galovic, "Photothermal Depth Profiling Of Optical Gradient Materials By Neural Network," *Publ. Astron. Obs. Belgrade*, vol. 89, no. May 2015, 2010.

[6] S. P. Djordjevic, K.Lj., Markushev, D.D., Ćojbašić, Ž. M., Galović, "Photoacoustic measurements of the thermal and elastic properties of n-type silicon using neural networks," *Silicon , Springer*.

[7] Y. LeCun, Y. Bengio, and G. Hinton, "Deep learning," *Nature*, vol. 521, no. 7553, pp. 436–444, 2015.

[8] S. Aleksic, D. Markushev, D. Pantic, M. Rabasovic, D. Markushev, and D. Todorovic, "Electro-acoustic influence of the measuring system on the photoacoustic signal amplitude and phase in frequency domain," *Facta Univ. - Ser. Physics, Chem. Technol.*, vol. 14, no. 1, pp. 9–20, 2016.

[9] A. Handa, V. Patraucean, V. Badrinarayanan, S. Stent, and R. Cipolla., "SceneNet: Understand- ing real world indoor scenes with synthetic data.," in *CVPR*, 2015.

[10] A. Shrivastava, T. Pfister, O. Tuzel, J. Susskind, W. Wang, and R. Webb, "Learning from Simulated and Unsupervised Images through Adversarial Training," in *2017 IEEE Conference on Computer Vision and Pattern Recognition (CVPR)*, 2017, pp. 2242–2251.

[11] G. Cosne *et al.*, "Using Simulated Data to Generate Images of Climate Change," in *ML-IRL workshop at ICLR*, 2020, pp. 1–9.

[12] M. I. Jordovic-Pavlovic *et al.*, "Computationally intelligent description of a photoacoustic detector," *Opt. Quantum Electron.*, vol. 52, no. 5, pp. 1–14, 2020.

[13] M. I. Jordović-Pavlović, M. M. Stanković, M. N. Popović, Ž. M. Ćojbašić, S. P. Galović, and D. D. Markushev, "The application of artificial neural networks in solid-state photoacoustics for the recognition of microphone response effects in the frequency domain," *J. Comput. Electron.*, vol. 19, no. 3, pp. 1268–1280, 2020.

[14] A. Rosencwaig, "Photoacoustic Spectroscopy of Solids," *Opt Commun, 7(4)*, pp. 305–308, 1973.

[15] L. C. M. Perondi, L. F, Miranda, "Minimal-Volume Photoacoustic Cell Measurement of Thermal Diffusivity: Effect of the Thermoelastic Sample Bending.," *J. Appl. Phys.*, vol. 62, pp. 2955–2959, 1987.

[16] M. Popovic, M. Nesic, S. Ciric-Kostic, M. Zivanov, D.Markushev, M. Rabasovic, S. Galovic, "Helmholtz Resonances in Photoacoustic Experiment with Laser-Sintered Polyamide Including Thermal Memory of Samples," *Int. J. Thermophys.*, vol. 37, no. 12, pp. 1–9, 2016.

[17] A. Rosencwaig and A. Gerscho, "Photoacoustic Effect with Solids: A Theoretical Treatment," *Science (80-.).*, vol. 190, pp. 556–557, Nov. 1975.

[18] F. A. McDonald and G. C. Wetsel, "Generalized theory of the photoacoustic effect," *J. Appl. Phys.*, vol. 49, no. 4, pp. 2313–2322, Apr. 1978.

[19] L. Rousset, F. Lepoutre, and L. Bertrand, "Influence of thermoelastic bending on photoacoustic experiments related to measurements of thermal diffusivity of metals," *J. Appl. Phys.*, vol. 54, no. 5, pp. 2383–2391, 1983.

[20] P. M. Nikolic and D. M. Todorović, "An investigation of semiconducting materials using a photoacoustic method. u: Technical sciences book 40, Monographs, Belgrade: Serbian Academy of Sciences and Arts Department, vol. DCXLVIII." Serbian Academy of Sciences and Arts, 2001.

[21] D. D. Markushev, M. D. Rabasović, M. V Nesic, M. N. Popovic, and S. P. Galovic, "Influence of thermal memory on thermal piston model of photoacoustic response," *Int. J. Thermophys.*, vol. 33, no.

10–11, pp. 2210–2216, 2012.

[22]   M. V Nesic, S. P. Galovic, Z. N. Soskic, M. N. Popovic, and D. M. Todorović, "Photothermal thermoelastic bending for media with thermal memory," *Int. J. Thermophys.*, vol. 33, no. 10–11, pp. 2203–2209, 2012.

[23]   S. P. Galovic, Z. N. Soskic, M. N. Popovic, Z. Stojanovic, D. Cevizovic, and Z. Stojanovic, "Theory of photoacoustic effect in media with thermal memory," *J. Appl. Phys.*, vol. 116, no. 2, pp. 0–12, 2014.

[24]   D. M. Todorović, M. D. Rabasovic, and D. D. Markushev, "Photoacoustic elastic bending in thin film—Substrate system," *J. Appl. Phys.*, vol. 114, no. 21, p. 213510, 2013.

[25]   D. M. Todorović, M. D. Rabasovic, D. D. Markushev, and M. Sarajlić, "Photoacoustic elastic bending in thin film-substrate system: Experimental determination of the thin film parameters," *J. Appl. Phys.*, vol. 116, no. 5, 2014.

[26]   M. Popovic, *Generalizovani fotoakustični odziv dvoslojnih struktura*. Beograd: Zadužbina Andrejević, 2018.

[27]   M. N. Popovic, "Fotoakustički odziv transmisione fotoakustičke konfiguracije i analiza rezonantnih fenomena za dvoslojne uzorke sa toplotnom memorijom," Univerzitet u Novom Sadu, 2016.

[28]   M. N. Popovic, D. D. Markushev, M. V. Nesic, M. I. Jordovic-Pavlovic, and S. P. Galovic, "Optically induced temperature variations in a two-layer volume absorber including thermal memory effects," *J. Appl. Phys.*, vol. 129, no. 1, 2021.

[29]   M. Popovic, M. Nesic, M. Zivanov, D. Markushev, and S. Galovic, "Photoacoustic response of a transmission photoacoustic configuration for two-layer samples with thermal memory," *Opt. Quantum Electron.*, vol. 50, p. 330, 2018.

[30]   M. D. Rabasovic, M. G. Nikolic, M. D. Dramicanin, M. Franko, and D. D. Markushev, "Low-cost, portable photoacoustic setup for solid samples," *Meas. Sci. Technol.*, vol. 20, no. 9, p. 95902, 2009.

[31]   M. Nesic *et al.*, "Development and comparison of the techniques for solving the inverse problem in photoacoustic characterization of semiconductors," *Opt. Quantum Electron.*, vol. 53, no. 7, p. 381, 2021.

[32]   Q. V Le, J. Ngiam, A. Coates, A. Lahiri, B. Prochnow, and A. Y. Ng, "On Optimization Methods for Deep Learning," in *Proceedings of the 28th International Conference on Machine Learning*, 2011, pp. 265–272.

[33]   Y. Bengio, "Practical recommendations for gradient-based training of deep architectures," *Lect. Notes Comput. Sci. (including Subser. Lect. Notes Artif. Intell. Lect. Notes Bioinformatics)*, vol. 7700 LECTU, pp. 437–478, 2012.

[34]   X. Glorot and Y. Bengio, "Understanding the difficulty of training deep feedforward neural networks," in *Proceedings of the Thirteenth International Conference on Artificial Intelligence and Statistics*, 2010, vol. 9, pp. 249–256.

[35]   D. P. Kingma and J. Ba, "Adam: {A} Method for Stochastic Optimization," *CoRR*, vol. abs/1412.6, 2014.